Journal of ELECTRICAL ENGINEERING, VOL 73(2022), NO1, 57–61

sciendo

COMMUNICATIONS

Pressure and humidity detector based on textile integrated waveguide

Martin Kokolia, Zbynek Raida[1]

In the paper, a pressure sensor and a humidity sensor are designed as supplementary components of a textile integrated waveguide (TIW) based on an artificial magnetic conductor (AMC) consisting of hexagonal elements. Thanks to AMC, sewing of electrically conductive side walls can be eliminated. Since operating in the stop-band of TIW, the sensors do not influence transmission parameters of TIW, and provide an additional functionality. For fabrication, a three-dimensional knitted fabric was used as a substrate and conductive surfaces were created from a self-adhesive copper foil. The sensors were simulated, manufactured and measured in the frequency range from 10 GHz to 12 GHz with a reasonable agreement. Since the designed components are sensitive on manufacturing tolerances, a higher measured insertion loss in TIW can be observed compared to simulations. Nevertheless, the insertion loss can be reduced when manufacturing accuracy is improved.

K e y w o r d s: textile-integrated waveguide (TIW), artificial magnetic conductor (AMC), pressure sensor, humidity sensor

1 Introduction

In the last decade, attention has been given to the integration of various electronic components and sensors into textile materials [1]-[3]. This approach promises seamless blending of functionality and comfort in both wearable applications and technical textiles, used inside vehicles typically [4]-[5]. Applications usually comprise DC and low frequency electronics, high frequency and microwave structures or even optoelectronical circuits or sonic sensors [6]-[11].

The RF sensing is the approach discussed in this paper. Since textile-integrated waveguides (TIW) constructed from artificial magnetic conductors (AMC) have already been used for a power transmission in vehicles, non-conventional sensors exploiting those structures are attractive being implemented with minimum costs [12].

Since TIW can be directly printed on a technical textile at upholstery of vehicles, savings of conventional cooper wiring and weight are associated with. TIW, which was presented in [13], operates at frequencies from 10 GHz to 12 GHz. If an optimal sensing system is going to be designed, no additional losses should be caused in power transmission on one hand, and a good sensing reliably should be ensured on the other hand.

At present, there are several approaches to sense physical changes inside and around the material adopting microwaves energy. Those approaches range from deformed waveguides [14], antennas receiving signal across the changing space [15], RFID systems [16] and related methods. Some work in this field was presented but most of devices are either too complex to be manufactured or only a single-purpose operation is provided.

In papers [14] and [17], the principle for sensing mechanical deformation caused by mechanical pressure is presented. In [14], authors presented a cavity resonator made of metal which wall was deformed at a certain level of high pressure outside the cavity. Thus, a dimension of the resonator and its resonant frequency were changed. In [15], authors described a coplanar waveguide made on a flexible substrate with several ring resonators. Once a certain mechanical deformation of the substrate occurred, properties of different resonators altered and the overall transmission of the structure was changed in a predictable way.

Another promising approach to implement a sensor structure utilizing microwave bands is described in [17] and [18]. In both papers, some kind of a cavity or a resonator is used. In the base state, the cut-off frequency or the resonant frequency can be observed from the viewpoint of frequency dependence of transmission coefficient. Given by known relative permittivity of an expected liquid and a variation of effective permittivity on the sensor, either the presence of different liquids can be detected or a change of liquids composition can be sensed.

The presented paper is aimed to utilize an artificial magnetic conductor (AMC)-based textile integrated waveguide (TIW) described in [13] for sensing. This TIW was designed to be used for power transmission in upholstery inside cars or airplanes. The straight section of the TIW is converted into a practical sensor with minimal modifications of the TIW while preserving the ease of manufacturing, low costs and the primary RF power transmission. Thus, the dual-purpose structure is created. As an example, two types of sensors were designed, manufactured, and tested in a controlled environment:

[1] Brno University of Technology, FEEC, Department of Radio Electronics, Technická 12, 616 00 Brno, Czechia, 146860@vut.cz, raida@vut.cz

https://doi.org/10.2478/jee-2022-0008, Print (till 2015) ISSN 1335-3632, On-line ISSN 1339-309X

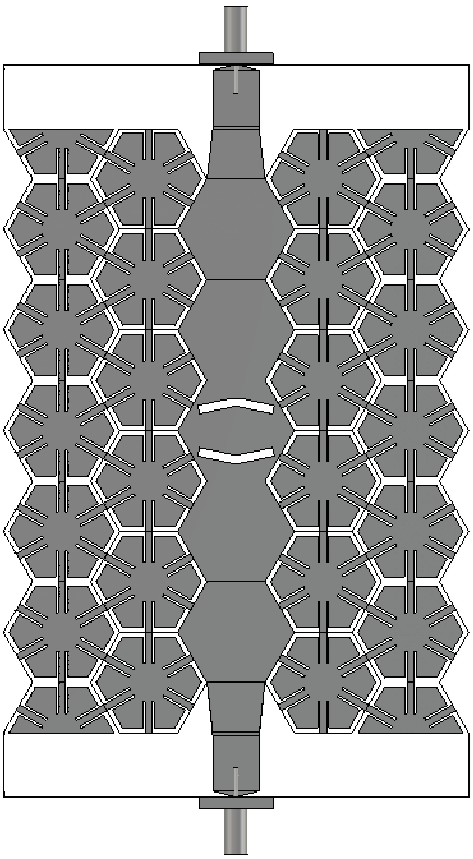

Fig. 1. AMC-based TIW. Side walls are replaced by two rows of hexagonal elements. The sensor is to be connected via the coupling slots in the TIW center. The structure is completed by SMA-to-microstrip transition at the input and the output

- The first sensor measures a variation of a textile thickness. Such a sensor can play the role of a user-interface button or can register the presence of a person on a seat.
- The second sensor detects the variation of relative permittivity. Such a device can sense the presence of water inside the textile. That way, the humidity inside the textile can be detected.

2 AMC based TIW sensors

Conventional textile-integrated waveguides (TIW) consist of a top and bottom conductive layer manufactured from a conductive fabric material, screen-printed silver paste, or a self-adhesive copper foil. Side walls can be sewed by a conductive thread. In order to eliminate the need of costly, time-demanding and inaccurate sewing, side walls can be replaced by an artificial magnetic conductor (AMC) as explained in [12].

The TIW was optimized to operate in the frequency range from 10 GHz to 12 GHz. The layout of the TIW was etched in a self-adhesive copper foil to be fixed to the 3D knitted textile SINTEX 3D097 ($h = 3.4\,\mathrm{mm}, \varepsilon_r = 1.2$). Proprieties of this material were investigated in [19]. Obviously, the manufactured TIW shows additional losses in comparison with the simulation of the lossless structure. A significant part of losses is due to the undesired radiation and dispersion at the edges of AMC cells at the transition from the feeding section to the straight section of TIW.

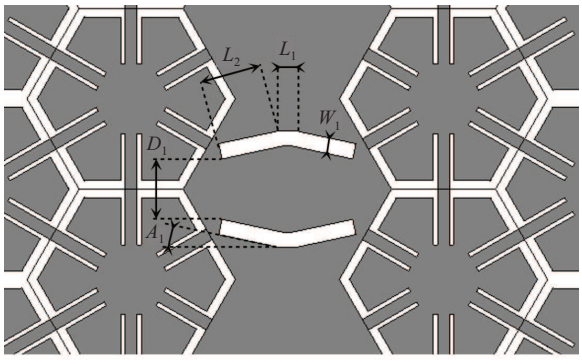

Fig. 2. Detail of coupling slots in the center of TIW

In order to find the resonance frequency, a resonator composed of a single hexagonal cell can be approximated by a rectangular cavity. The physical length of the cell is 17.4 mm but the effective length is smaller since the virtual electrical wall is not perfectly thin and causes an extension within <0.50 mm; 0.75 mm$>$ inwards. Hence, the approximate resonance frequency is f = 8.6 GHz. The AMC-based waveguide operates with TE00 mode and the cavity resonator operates with TE001 mode. In Fig. 3, absolute value of E-field intensity is shown at the operation frequency f = 8.6 GHz. Progressively changing shape of the wave traveling thought the waveguide is the result of the changing velocity of propagation at different angles of coincidence with the AMC cell walls. At frequencies between 10 GHz and 12 GHz, the TE002 mode is excited inside the cavity resonator with minima placed around feeding slots. Thus, the minimal energy returns to the waveguide and the propagating wave is not interfering with.

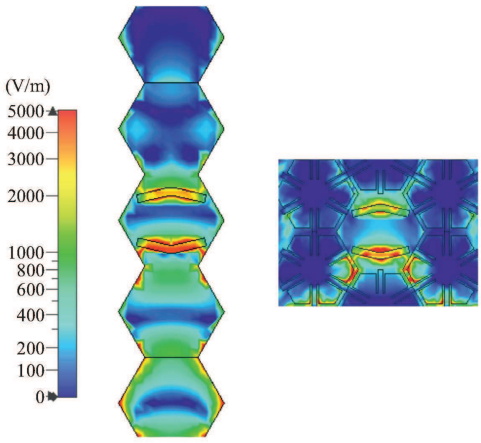

Fig. 3. Absolute value of E-field intensity at f = 8.63 GHz inside TIW (left). Detail of coupling slots (right)

Table 1. Dimensions of coupling slots of TIW

Variable	Value	Unit
A1	12.5	degrees
D1	5.8	mm
W1	2.0	mm
L1	1.5	mm
L2	6.0	mm

Table 2. Dimensions of sensing slots of humidity detector

Variable	Value	Unit
D2	2.50	mm
L2	12.00	mm
W2	2.50	mm

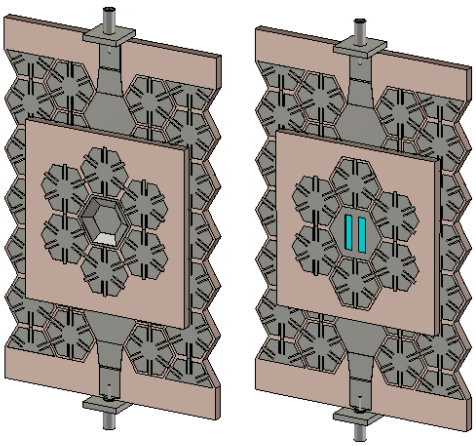

Fig. 4. AMC-TIW pressure sensor at maximum deformation (left). AMC-TIW humidity detector (right)

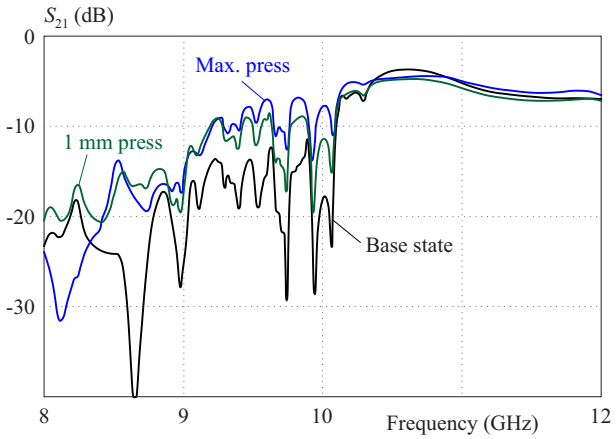

Fig. 5. Simulated frequency response of transmission coefficient of the pressure sensor

The sensors to be coupled to TIW via coupling slots are conceived as cavity resonators consisting of a single AMC cell. Side walls of the resonators are created by a single row of AMC cells to eliminate the need of sewing. Both the sensors are shown in Fig. 4. The precise alignment of feeding slots in TIW and the cavity resonator of the sensor is critical for an efficient operation of the system. In real situations, random stop bands or a slight frequency shift of the stop band might appear. Since the negligible influence on the communication within the band from 10 GHz to 12 GHz is requested, the change of losses in the stop band should be consistent across the whole range of deformations and permittivity variations.

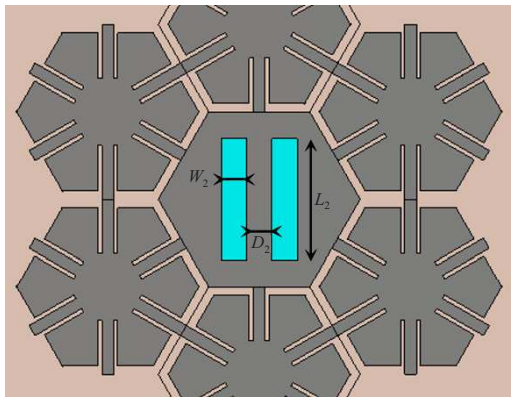

Fig. 6. Dimensions of sensing slots of the humidity detector

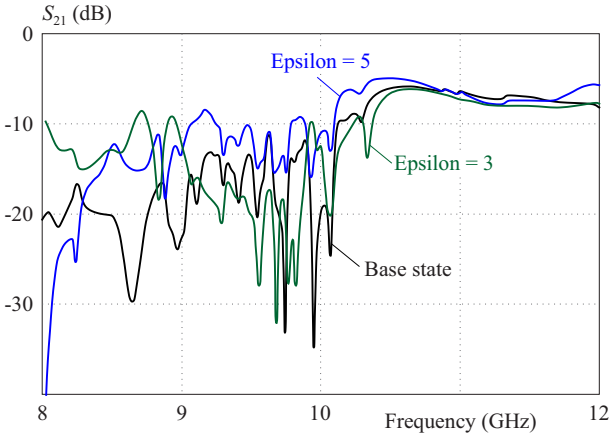

Fig. 7. Simulated frequency response of transmission coefficient of the humidity detector

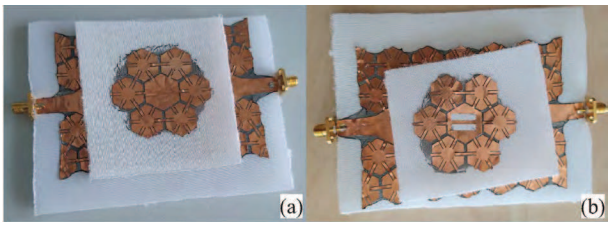

Fig. 8. Manufactured prototypes of the pressure sensor (left) and the humidity detector (right)

Figure 7 shows simulated losses between ports of the waveguide with the humidity detector. The difference between frequency characteristics of the initial state with

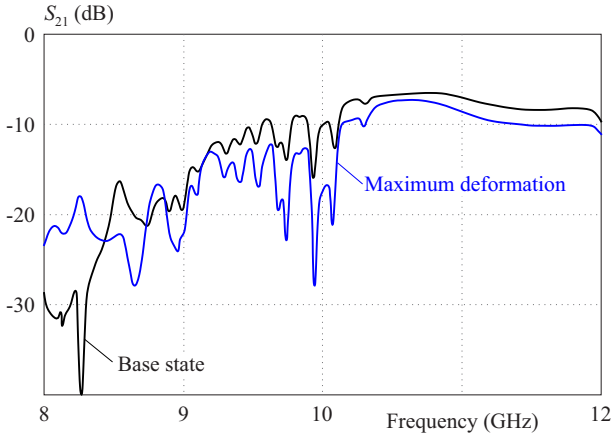

Fig. 9. Measured frequency response of transmission coefficient of the pressure sensor

the dry textile and an expected threshold humidity inside the textile is obvious. The most significant and reliable variation in the range of parametric analysis can be seen at 8.65 GHz. In the simulated range of relative permittivity inside the cavity, the peak of the stop band at this frequency was only diminishing with no other peak that could be misinterpreted.

3 Manufacturing and testing

Results show that the desired stop band is less pronounced and appears at a slightly lower frequency 8.25 GHz. When pressed, the losses at 8.25 GHz are lessened by 20 dB, making this change quite significant (at very narrow frequency band). For example, the change is only about 10 dB at 8.20 GHz. On the other hand, the communication band from 10.0 GHz to 12.0 GHz is not disturbed at all. %Fig. 10 Measured frequency response of transmission coefficient of the humidity detector.

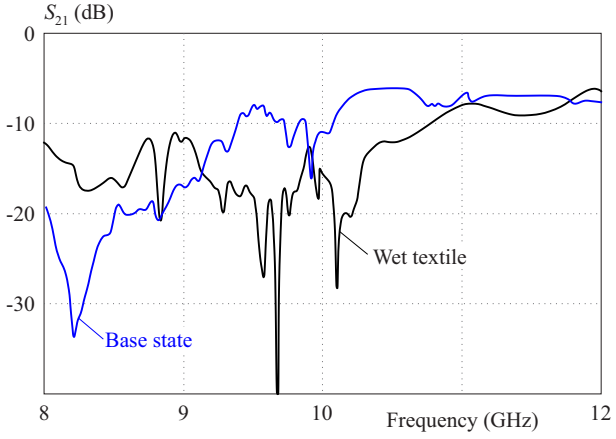

Fig. 10. Measured frequency response of transmission coefficient of the humidity detector

Few drops of a pure water were dropped at the central element of the detector to test the functionality. Results show that the real response of the humidity detector is very similar to simulation. Roughly at 8.2 GHz, there is a pronounced peak of losses at the initial state. When the humidity was present, the losses at this frequency significantly diminished and the stop band disappeared. This makes the effect of the humidity hard to mistake and proves the concept of the sensor. The communication band from 10.0 GHz to 12.0 GHz is visibly disturbed in its lower part, and there is a reasonably small increase in losses from 10.8 GHz to 12.0 GHz. This could be contributed to water getting into the waveguide in the lower layer of the textile. The tested prototype was dried naturally and tested again. When enough water was added to be detectable clearly, the results were similar.

4 Conclusions

In the paper, the concept of the pressure sensor and the humidity detector coupled to the textile integrated waveguide is presented. The AMC-based waveguide was used for the communication in the frequency band from 10.0 GHz to 12.0 GHz. For sensing and detection, a lower frequency band from 8.0 GHz to 10.0 GHz was used. Hence, a dual-purpose system was designed. At lower frequencies, sensor applications were implemented while minimizing effects on power transmission within the communication frequency band. The design comprises a cavity resonator to be put on the top of the waveguide. Resonant frequency of the resonator is varied by the change of thickness of the textile substrate (in case of the pressure sensor) or by the change of permittivity (in case of the humidity detector). The sensors were manufactured and tested in realistic conditions. Transitions of textile integrated waveguides were measured by a vector network analyzer while sensing was applied. The pressure sensor was used as a button. The realistic maximal deformation was about half of the thickness of the textile without the permanent damage. Due to higher losses in the communication band, the stop band used for sensing is very pronounced. At 8.25 GHz, there was a stop band peak very pronounced completely absent, when the sensor was pressed. Results provided by testing of humidity detector are also somewhat different from the expected response since the control of the precise distribution of the water inside the desired sensing section is difficult. This could be mitigated in further development. Nevertheless, the detection capability at 8.2 GHz was very strong and reliable.

Acknowledgment

The presented research was supported by the Internal Grant Agency of Brno University of Technology (the project no. FEKT-S-20-6526). The research is part of the project FV40385 Textile electronics for homecare and professional use (TED) funded by Czech Ministry of Industry and Trade.

References

[1] W. He, C. Wang, H. Wang, M. Jian, W. Lu, X. Liang, X. Zhang, F. Yang, and Y. Zhang, "Integrated Textile Sensor Patch for Real–Time and Multiplex Sweat Analysis", *Science Advances*, vol. 5, no. 11, pp. 1–8, 2019.

[2] D. Teichmann, A. Kuhn, S. Leonhardt, and M. Walter, "The Main Shirt: A Textile–Integrated Magnetic Induction Sensor Array", *Sensors*, vol. 14, no. 1, pp. 1039–1056, 2014.

[3] A. V. Cioffi, A. Raffo, and S. Costanzo, "Preliminary Validations of Textile Wearable Microwave Sensor for Biomedical Applications", *13th European Conference on Antennas and Propagation*, Krakow vol. , no. Poland, IEEE, 2019.

[4] M. Cupal *et al*, "Textile–Integrated Electronics for Small Airplanes", *12th European Conference on Antennas and Propagation*, London vol. , no. UK, IEEE, 2018.

[5] C. Loss, C. Gouveia, R. Salvado, P. Pinho, and J. Vieira, "Textile Antenna for Bio–Radar Embedded in a Car Seat", *Materials*, vol. 14, no. 1, pp. 1–18, 2021.

[6] C. Ataman, T. Kinkeldei, G. Mattana, A. V. Quintero, F. Molina–lopez, J. Courbat, K. Cherenack, D. Briand, G. Trster, and N. F. d. Rooij, "Robust Platform for Textile Integrated Gas Sensors", *Sensors & Actuators B: Chemical*, vol. 177, pp. 1053–1061, 2013.

[7] Y. J. Yun, W. G. Hong, N. J. Choi, B. H. Kim, Y. Jun, and H. K. Lee, "Ultrasensitive and Highly Selective Graphene–Based Single Yarn for Use in Wearable Gas Sensor", *Scientific Reports*, vol. 5, no. 1, article pp, 10904, 2015.

[8] T. Kinkeldei, C. Zysset, K. H. Cherenack, and G. Troster, "A Textile Integrated Sensor System for Monitoring Humidity and Temperature", *16th International Conference on Solid–State Sensors, Actuators and Microsystems*, Beijing vol. , no. China, IEEE, 2011.

[9] C. Zysset, N. Nasseri, L. Bthe, N. Mnzenrieder, T. Kinkeldei, L. Petti, S. Kleiser, G. A. Salvatore, M. Wolf, and G. Trster, "Textile Integrated Sensors and Actuators for Near–Infrared Spectroscopy", *Optics Express*, vol. 21, no. 3, pp. 3213–3224, 2013.

[10] J. Tabor, T. Agcayazi, A. Fleming, B. Thompson, A. Kapoor, M. Liu, M. Y. Lee, H. Huang, A. Bozkurt, and T. K. Ghosh, "Textile–Based Pressure Sensors for Monitoring Prosthetic–Socket Interfaces", *IEEE Sensors Journal*, vol. 21, no. 7, pp. 9413–9422, 2021.

[11] S. K. Bahadir, F. Kalaoglu, S. Thomassey, I. Cristian, and V. Koncar, "A Study on the Beam Pattern of Ultrasonic Sensor Integrated to Textile Structure", *ternational Journal of Clothing Science and Technology*, vol. 23, no. 4, pp. 232–241, 2011.

[12] M. Kokolia, "Hexagonal–Cell Artifical Magnetic Conductor Waveguide", *ternational Conference on Microwave Techniques*, Pardubice (Czech Rep,): IEEE, 2019.

[13] M. Kokolia and Z. Raida, "Textile-Integrated Microwave Components Based on Artificial Magnetic Conductor", *ternational Journal of Numerical Modelling*, vol. 34, no. 4, 2021.

[14] H. Kou, Q. Tan, Y. Wang, G. Zhang, S. Shujing, and J. Xiong, "A Microwave SIW Sensor Loaded with CSRR for Wireless Pressure Detection in High–Temperature Environments", *Journal of Physics. D: Applied Physics*, vol. 53, no. 8, pp, 85101, 2019.

[15] C. Arenas–Buendia, F. Gallee, A. Valero–Nogueira, and C. Person, "RF Sensor Based on Gap Waveguide Technology in LTCC for Liquid Sensing", *9th European Conference on Antennas and Propagation*, Lisbon vol. , no. Portugal, IEEE, 2015.

[16] U. H. Khan, B. Aslam, M. A. Azam, Y. Amin, and H. Tenhunen, "Compact RFID Enabled Moisture Sensor", *Radioengineering*, vol. 25, no. 3, pp. 449–456, 2016.

[17] J. Naqui, M. Durn–Sindreu, and F. Martn, "Alignment and Position Sensors Based on Split Ring Resonators", *Sensors*, vol. 12, no. 9, pp, 11790, 2012.

[18] M. Sameer and P. Agarwal, "Coplanar Waveguide Microwave Sensor for Label–Free Real–Time Glucose Detection", *Radioengineering*, vol. 28, no. 2, pp. 491–495, 2019.

[19] M. Kokolia and Z. Raida, "Milimeter–Wave Propagation in 3D Knitted Fabrics", *22nd International Microwave and Radar Conference*, Poznan vol. , no. Poland, IEEE, 2018.

[20] D. Elsheikh and A. R. Eldamak, "Microwave Textile Sensors for Breast Cancer Detection", *National Radio Science Conference*, Mansoura vol. , no. Egypt, IEEE, 2021.

[21] M. E. Gharbi, R. Fernndez–Garca, and I. Gil, "Textile Antenna–Sensor for In Vitro Diagnostics of Diabetes", *Electronics*, vol. 10, no. 13, 2021.

[22] F. Nikbakhtnasrabadi, H. E. Matbouly, M. Ntagios, and R. Dahiya, "Textile–Based Stretchable Microstrip Antenna with Intrinsic Strain Sensing", *ACS Applied Electronic Materials*, vol. 3, no. 5, pp. 2233–2246, 2021.

[23] M. E. Gharbi, M. Martinez–Estarada, R. Fernndez–Garca, and I. Gil, "Determination of Salinity and Sugar Concentration by Means of a Circular–Ring Monopole Textile Antenna–Based Sensor", *IEEE Sensors Journal*, vol. 21, no. 21, pp. 23751–23760, 2021.

[24] J. A. Toro, W. F. M. Granada, and S. M. Y. Zuluaga, "Design and Implementation of a Wearable Patch Antenna that Serves as a Longitudinal Strain Sensor", *Textile Research Journal*, 2021.

[25] M. Roudjane, S. Bellemare–Rousseau, E. Drouin, B. Belanger–Huot, M. A. Dugas, A. Miled, and Y. Messaddeq, "Smart T–Shirt Based on Wireless Communication Spiral Fiber Sensor Array for Real–Time Breath Monitoring: Validation of the Technology", *IEEE Sensors Journal*, vol. 20, no. 18, pp. 10841–10850, 2020.

[26] M. Roudjane, M. Khalil, H. Abed, A. Miled, and Y. Messaddeq, "Wearable Scanner Platform Based on Fiber Sensor Array for Real Time Breath Detection", *18th IEEE International Conference on New Circuits and Systems*, Montreal vol. , no. Canada, IEEE, 2020.

[27] G. Atanasova and N. Atanasov, "Small Antennas for Wearable Sensor Networks: Impact of the Electromagnetic Properties of the Textiles on Antenna Performance", *Sensors*, vol. 20, no. 18, pp. 1–21, 2020.

[28] S. Costanzo and V. Cioffi, "Preliminary SAR Analysis of Textile Antenna Sensor for Non–Invasive Blood–Glucose Monitoring", *Advances in Intelligent Systems and Computing*, vol. 1137 AISC, pp. 607–612, 2020.

[29] S. Ghosh, B. Nitin, S. Remanan, Y. Bhattacharjee, A. Ghorai, T. Dey, T. K. Das, and N. C. Das, "A Multifunctional Smart Textile Derived from Merino Wool/Nylon Polymer Nanocomposites as Next Generation Microwave Absorber and Soft Touch Sensor", *ACS Applied Materials and Interfaces*, vol. 12, no. 15, pp. 17988–18001, 2020.

[30] B. D. Wiltshire, K. Mirshahidi, A. V. Nadaraja, S. Shabanian, R. Hajiraissi, M. H. Zarifi, and K. Golovin, "Oleophobic Textiles with Embedded Liquid and Vapor Hazard Detection Using Differential Planar Microwave Resonators", *Journal of Hazardous Materials*, vol. 409, 2021.

Received 28 October 2021